Spatio-temporal organization of colloids in start-up flows

Nicos S. Martys[1], Didier Lootens[2], William George[1], and Pascal Hébraud[3]

[1] *National Institute of Standards and Technology, 100 Bureau Drive, Stop 8615, Gaithersburg, MD 20899-8615, USA*

[2] *SIKA Technology A.G., Tuffenwies 16, CH-8048 Zürich, Switzerland*

[3] *IPCMS UMR* 7504 *23 rue du Loess 67034 Strasbourg Cedex 02, France*

Spatio-temporal correlations in start-up flows of attractive colloids are explored by numerical simulations, as a function of their volume fraction and shear rate. The suspension is first allowed to flocculate during a time t_w, then the stress necessary to induce its flow is computed. We show that the start-up flow of these suspensions can be characterized by the creation, orientation and disruption of contacts between particles. Whereas at low volume fractions, the stress is a universal function of the deformation, at high volume fractions, scaling behavior is no longer observed and a supplementary stress becomes necessary at equivalent shear rates. Our simulations show that the onset of flow is dominated by the creation of contacts between the particles at low shear rates, and by their disruption at high shear rates. Under flow, the contacts between colloids become strongly anisotropic. When the contacts are oriented in the compression gradient of the shear flow, a supplementary stress is necessary to induce the flow.

PACS numbers: 83.80.Hj,87.10.Tf,83.60.Df

Macroscopic flow properties of complex fluids result from the organization of their constituents. For simple enough systems, the microstructure at rest and under flow may be calculated and related to their macroscopic rheological properties, *e.g.* the rheological behavior of polymer solutions and blends is generally understood [1]. However, for non equilibrium systems, the description of their structure either at rest or under flow is much more involved. Semi-phenomenological models have been developed to describe the flow behavior of soft glassy materials [2] both under transient or constant flow [3]. Simulations and experiments have been performed to observe the microstructure of colloidal suspensions [4, 5], and aggregated colloidal suspensions [6, 7] under constant flow. Nevertheless, the initial establishment of this microstructure is much more difficult to study, mainly because experimental observation techniques, such as light or neutron scattering techniques, require long averaging times. Mechanical measurements show that there may exist, for soft glassy systems, a very non-linear relationship between the applied stress and the induced shear deformation or shear rate deformation. While it is generally observed that the system starts to flow only under the application of a non-zero value of the stress : the yield stress [9], the value, the measurement, and even the existence of yield stress are not well established [10]. Recent experiments tend to show that some fluid zones are always present in disordered materials, so that the system flows at very small stresses. Theoretical description of the onset of flow is made difficult by the fact that the cooperative motion of the system constituents must be described. Regardless, it is of crucial importance to understand how these materials start to flow and to tune their physicochemical properties in order to reduce the amount of energy necessary to make them flow. For instance, the energy necessary to make a cement suspension flow is greatly reduced by using dispersing polymeric additives [11].

In this Letter, we use a dissipative particle dynamics (DPD) model to study the onset of flow of a colloidal suspen-

sion of attractive particles. We model the flow of a concentrated suspension similar to spherical alumina particles of approximately 100 nm diameter. The interaction potential between two particles exhibits a minimum of 25 k_BT at a distance of 6 nm between the surfaces of the particles. The DPD simulation is similar to molecular dynamics simulation, but, instead of modeling all the molecular properties of the system, mesoscopic particles are considered [13, 14]. These particles are subjected to conservative, dissipative and random forces. In order to satisfy the fluctuation-dissipation theorem, the last two forces are related. The conservative force is utilized to control the compressibility of the system, so that it matches that of water [12]. Besides forces acting on mesoscopic particles, an additional interaction potential is applied to the colloids : at short distances, this potential scales as the sum of a hard sphere repulsion term, A_{HS}/r^8 and a Van der Waals potential, H/r^2, where H is the Hamaker constant. The colloid's radius is the only length scale explicitly included in the description of the suspension. The colloidal particles are attractive, and in the absence of flow, the suspension evolves to form a colloidal attractive gel. We thus follow a well-defined preparation protocol of the suspension. It is prepared by randomly placing the spheres, in a cubic cell, with small overlaps being possible. Then, a repulsive force is applied between spheres if they overlap. Once all the spheres no longer overlap, the system is allowed to equilibrate under the action of Brownian and hydrodynamic forces. When a stable radial distribution function is obtained, the Van der Waals and lubrication forces are introduced by turning them on slowly enough so that the kinetic energy that is introduced in the system because two spheres are too close each other, is allowed to dissipate. We choose the end of the introduction of the van der Waals and the lubrication forces as the initial time of the system. Then, for a given time t_w, the suspension is allowed to evolve towards a flocculated colloidal gel. As the suspension ages during a time t_w, it is still out of equilibrium, and during this period, the number of contacts between particles increases [15]. At several t_w values, we then begin to make the suspension flow. A shear flow is imposed by translating the upper and lower boundaries of the cube. The direction of the flow is denoted $\mathbf{u_x}$ and its gradient $\mathbf{u_y}$. We study three volume concentrations, $\phi = 20$ %, 40 % and 50 % where the number of collodial particles range from 3760 to 9616. As the interparticle interaction is strong, the relevant energy scale in our system is the interaction potential between two particles, rather than thermal energy, so that in the studied flow regime the interaction forces between two particles compete with hydrodynamic forces. Given that $F_{\max}$ is the maximal interaction force between two colloids, a their radius, η the viscosity of the continuous medium, the natural stress, shear rate (and thus also time) units of our flow are given by :

$$\sigma = \phi^2 \frac{F_{max}}{a^2} \tag{1}$$

$$\dot{\gamma} = \frac{F_{max}}{6\pi\eta a^2} \tag{2}$$

where σ is the product of $F_{\max}$ with the number of particle bonds that cross the unit area, ϕ^2/a^2 [16], $\dot{\gamma}$ is the shear rate, that equilibrates the intercolloidal stress, $F_{\max}/a^2$, with the hydrodynamic stress, $6\pi\eta\dot{\gamma}$. Our simulation results may thus be compared to real systems in which the energy of interactions between colloids is larger than thermal energy. Considering 100 nm alumina particles, the maximal interaction force, given by the maximum of the slope of the interaction potential is of the order of 4.10^{-13} N, so that the corresponding stress scale is 40 Pa. The corresponding shear rate regime we study ranges from 6 to 600 s^{-1}. Once a stationary flow is reached, a shear-thinning behavior is observed : the stress, σ, is a power-law function of the shear rate, $\dot{\gamma}$, whose slope is 0.55 ± 0.05 (fig. 1d). With our dimensionless units, all the stress values superimpose. At the highest shear rate, the reduced stress corresponding to the 50 % volume fraction is $\sim$ 25 % higher than the one for the lower two volume fractions. In the stationary

flow regime, flocculation of the particles has been erased by the flow, and the flow properties of the suspension does not depend on the equilibrium time t_w. This non-Newtonian behavior has been observed in the flow of attractive colloidal suspensions, and is associated with the disruption of the aggregates at low shear and to the organization of the particles in planes, parallel to the direction of flow, that slide one over the other [5]. In contrast, the transient regime of stress establishment not only depends on the suspension concentration, but also on the equilibrium time.

For the smallest studied concentration, $\phi = 20$ %, and at the smallest shear rate, the stress progressively increases to a maximum value that does not strongly depend on the equilibrium time. *A contrario*, the value of the stress at the **starting** of its application depends on the equilibrium time : the longer t_w, the higher the initial stress value. Nevertheless, all the curves follow a master curve behavior and superimpose when plotted as a function of $t - t_w$ (fig. 1). Such self-similarity is characteristic of the aging dynamics of out of equilibrium systems, and has been observed in the case of concentrated soft colloidal particles [8]. The application of flow plays the same qualitative role as the aging of the suspension.

On the contrary, for the highest concentrations studied, when the waiting time is long enough, the evolution of the stress as a function of time exhibits a different shape and the curves may no longer be superimposed. At long waiting times, the value of the stress at null deformation tends now towards a non-zero finite value. The stress needed to make the suspension flow exceeds the one that would be necessary according to the aging behavior. This departure from the scaling behavior occurs once the flow of the suspension has been started, but before the establishment of a stationary regime. The excess of stress, relative to the scaling behavior, needed to make the suspension flow thus differs from the idealized concept of yield stress, which is a non-zero value of the stress required to induce the flow, as $\dot{\gamma} \longrightarrow 0$, and we call this excess stress a "supplementary stress". The higher the suspension concentration and the higher the shear rate, the greater the supplementary stress needed.

We need to describe the microstructure of the suspension responsible for the supplementary stress. The pair distribution function, $g(r)$, of the suspension exhibits a first peak at contact, near $r = 2a$, and a series of 2 correlation peaks. As the stress is localized in the thinnest gaps between particles [17], we focus our analysis on the particles in near contact and consider the pair distribution function $g(r)$ of the suspensions, at different times after the application of stress. $g(r)$ exhibits a well-defined maximum at $r = 2a$, when the particles are at contact. From the value of this maximum, one can compute the average number of contacts Z of the particles :

$$Z = \frac{N}{V} \int_{2a}^{2a+\delta a} 4\pi r^2 g(r) dr \tag{3}$$

a being the radius of the particles, δa the width of the first peak of the pair distribution function, N their number and V the volume of the shearing cell. In the absence of flow, whatever the volume fraction, the number of contacts increases with time. It tends towards a plateau value close to 7. The higher the concentration and the longer the equilibrium waiting time, the faster is the plateau value of Z reached. At low shear rates, the number of contacts increases with time. On the contrary, at high shear rates, the total number of contacts decreases as time elapses, before reaching an equilibrium. Whatever the applied shear rate value, the evolution of the number of contacts as a function of the accumulated deformation follows a simple exponential behavior (Fig. 2). Thus, there exists a characteristic strain γ_c of contact formation (at low shear rate), or contact disruption (at high shear rates). At low shear rate, γ_c is of the order of 100 %, corresponding to the characteristic shear necessary to induce collision between two colloids. γ_c thus decreases when the volume fraction of the suspension increases (Fig. 2d). In contrast, at higher shear rates,

the number of contacts decreases, and disruption of contacts dominates the dynamics, and γ_c no longer depends on the volume fraction of the suspension (Fig. 2d). Whatever the volume fraction and the shear rate, the evolution of the number of contacts as a function of deformation is always a simple exponential function and we do not observe any increase of the contact number that could be responsible for the appearance of a supplementary stress when the suspension has aged long enough.

By considering the orientation of the pairs of particles in contact, one sees a very different behavior at low and at high volume fractions and shear rates. We do not observe any orientation of the direction of contacts either in the plane normal to the shear direction, or in the plane normal to the shear. In the shear/shear gradient plane, the contacts become strongly anisotropic under flow (fig. 3). At low volume fractions, contacts form at a positive angle from the flow direction, in the extension quadrant of the shear flow. On the contrary, at high volume fractions and increasing shear rates, the number of contacts decreases in the extension quadrant of the shear flow, and increases in the compression quadrant (fig. 3). This observation agrees with experimental observation of the formation of aggregates in the compression quadrant, close to the direction of the flow [5]. As a consequence, the stress tensor σ_{ij}, which may be related to a microstructure tensor μ_{ij} with a linear relationship, $\sigma_{ij} = \eta\mu_{ij}(\dot{\gamma})\dot{\gamma}$, exhibits opposite symmetries at low and high volume fractions. Thus, the first normal stress difference, N_1, defined as the difference between the normal stress in the gradient and in the flow directions, changes sign when the volume fraction increases (Fig. 4). At low shear rates, N_1 is negative at $\phi = 20$ % and its absolute value increases with the amplitude of the deformation up to $\gamma = 0.7$ (Fig. 4a). Conversely, at $\phi = 50$ %, N_1 strongly fluctuates and generally becomes positive (Fig. 4b).

This observation of large first normal stress difference fluctuations at low shear rates and high volume fractions is in agreement with our initial hypothesis that the rheological properties of the suspension are dominated by the contacts between particles and their orientation relative to the shear. Normal stress fluctuations are indeed due to changes in the local arrangements of the contacts in the sheared suspension. The microstructure of the suspension thus depends strongly on the volume fraction and the applied shear rate. These results are in agreement with experimental observations of the flow of concentrated colloidal silica suspensions [18, 19]. Nevertheless, those experiments were performed in the regime where a stationary flow is established. Our numerical simulations show moreover that the microstructure develops at shear amplitudes smaller than unity, and that normal stress fluctuations occur at the onset of the application of flow. These positive values of the first normal stress difference are due to the increase of volume necessary to let the contacts reorganize : the suspension becomes dilatant.

In summary, the beginning of the application of a shear flow to a colloidal suspension induces an anisotropy of the organization of the particles. This anisotropy is qualitatively different at low and high volume fractions. In the first case, an excess of particles develop, whose relative orientation lies in the extension quadrant of the shear flow, in the latter, there is an increase of particles whose relative orientation is in the compression quadrant. This anisotropy of particles contacts has strong consequences on the rheological properties of the suspension at the onset of flow : it is associated with the appearance of a supplementary stress at very low shear amplitudes and of the dilatancy of the suspension.

Acknowledgements We would like to gratefully acknowledge support from the Virtual Cement and Concrete testing Laboratory consortium (VCCTL). The flow simulations were performed under award SMD-05-A-0129, "Modeling the Rheological Properties of Suspensions : Applications to Cement Based Materials" for NASA's National Leadership Computing System Initiative on the "Columbia" supercomputer at the NASA Ames Research Center.

---

[1] M. Doi and S.F. Edwards The theory of polymer dynamics. *Oxford University Press*, 1986.

[2] P. Sollich, F. Lequeux, P. Hébraud, and M.E. Cates Rheology of soft glassy materials. *Physical Review Letters*, 1996.

[3] P. Sollich Rheological constitutive equation for a model of soft glassy materials. *Physical Review E*, **58**, *1*, 738-750, 1998.

[4] P. Varadan and M.J. Solomon Direct visualization of flow-induced microstructure in dense colloidal gels by confocal laser scanning microscopy. *Journal of Rheology*, **47**, *4*, 943-968, 2003.

[5] B.J. Maranzano and N.J. Wagner Flow-small angle neutron scattering measurements of colloidal dispersion microstructure evolution through the shear thickening transition. *Journal of Chemical Physics*, **117**, *22*, 10291-10302, 2002.

[6] W. Wolthers, D. van den Ende, V. Breedveld, M.H.G. Duits, A.A. Potanin, R.H.W. Wientjes and J. Mellema Linear viscoelastic behavior of aggregated colloidal dispersions. *Physical Review E*, **56**, *5*, 5726-2733, 1997.

[7] T. Serra, J. Colomer and X. Casamitjana Aggregation and breakup of particles in a shear flow. *Journal of Colloids and Interface Science*, **187**, 466-473, 1997.

[8] M. Cloitre, R. Borrega and L. Leibler Rheological aging and rejuvenation in microgel pastes. *Physical Review Letters*, **85**, *22*, 4819-4923, 2000.

[9] R.G. Larson The structure and rheology of complex fluids. *Oxford University Press*, New York, 1999.

[10] P.C.F. Møller, J. Mewis and D. Bonn Yield stress and thixotropy : on the difficulty of measuring yield stresses in practice. *Soft Matter*, **2**, 274-283, 2006.

[11] R.J. Flatt, N. Martys and L. Bergstrom The rheology of cementitious materials. *MRS Bulletin*, **29**, *5*, 314-318, 2004.

[12] R.D. Groot and P.B. Warren Dissipative particle dynamics : Bridging the gap between atomistic and mesoscopic simulation. *Journal of Chemical Physics*, **107**, 4423-4435, 1997.ue hannong

[13] P.J. Hoogerbrugge and J.M.V.A. Koelman Simulating microscopic hydrodynamic phenomena with dissipative particle dynamics. *Europhysics Letters*, **19**, 155160, 1992.

[14] N.S. Martys Study of a dissipative particle dynamics based approach for modeling suspensions. *Journal of Rheology*, **49**, *2*, 401-424, 2005.

[15] R.J.M. d'Arjuzon, W. Frith and J.R. Melrose Brownian dynamics simulations of aging colloidal gels. *Physical Review E*, **67**, 06104, 2003.

[16] W.B. Russel, D.A. Saville and W.R. Schowalter Colloidal Dispersions. *Cambridge University Press*, 1989.

[17] L.E. Silbert, R.S. Farr, J.R. Melrose and R.C. Ball Stress distributions in flowing aggregated colloidal suspensions. *Journal of Chemical Physics*, **111**(10), 4780-4789, 1999.

[18] D. Lootens, H.Van Damme, and P. Hébraud. Giant stress fluctuations at the jamming transition. *Physical Review Letters*, **90**, 178301, 2003.

[19] D. Lootens, H. van Damme, Y. Hémar and P. Hébraud Dilatant flow of concentrated suspensions of rough particles. *Physical Review Letters*, **95**, 268302, 2005.

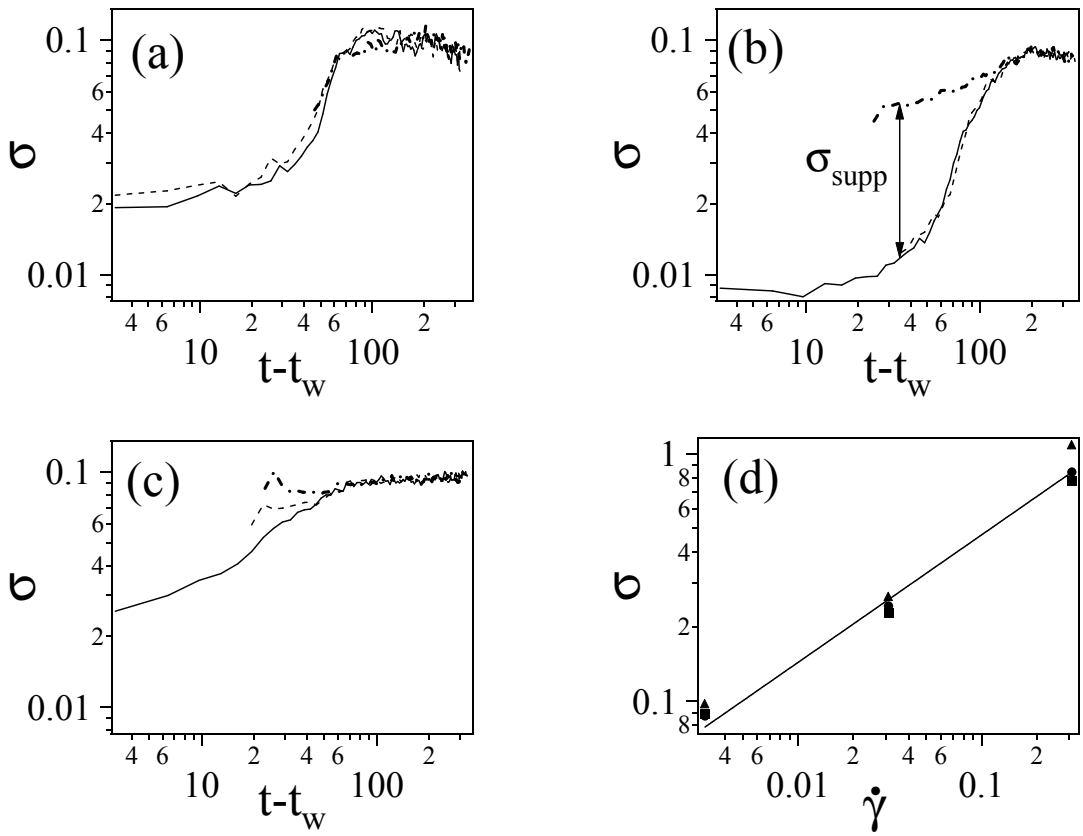

FIG. 1: **(a),(b),(c)** Dimensionless stress as a function of time when a constant shear rate is applied ($\dot{\gamma} = 3.5.10^{-3}$). **(a)** $\phi = 20$ %, **(b)** $\phi = 40$ %, **(c)** $\phi = 50$ %. Before the application of shear, the suspension rests for a time $t_w = 9.3$ (continuous line), $t_w = 93$ (dashed line), or $t_w = 1120$ (bold dashed line). When the time scale is translated by t_w, all the curves superimpose at low concentration, and exhibit a supplementary stress σ_{supp} at the two most concentrated concentrations. **(d)** Stress as a function of the shear rate in the equilibrium flow regime. $\phi = 20$ % (•), $\phi = 40$ % (■) and $\phi = 50$ % (▲). The continuous line is a guide to the eye, of slope 0.5.

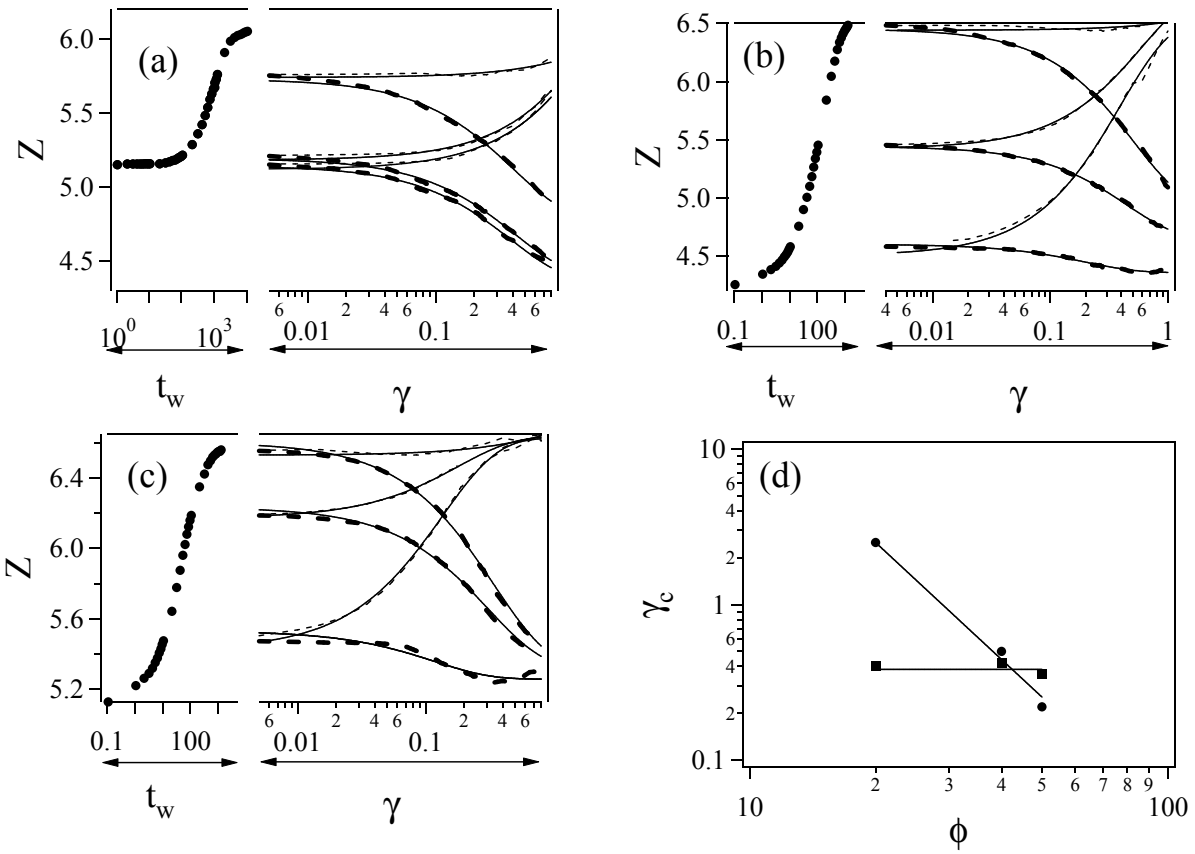

FIG. 2: Evolution of the number of contacts as a function of t_w, before the application of shear rate (•), and under flow as a function of the accumulated deformation, for three volume fractions, $\phi = 20$ % ((**a**)), $\phi = 40$ % ((**b**)) and $\phi = 50$ % ((**c**)). Two shear rate values are represented : $\dot{\gamma} = 3.5.10^{-3}$ (thin dashed lines) and $\dot{\gamma} = 3.5.10^{-1}$ (thick dashed lines). Continuous lines are exponential fits of the data. **(d)** Critical shear rates deduced from the monoexponential fits, at $\dot{\gamma} = 3.5.10^{-3}$ (•) and $\dot{\gamma} = 3.5.10^{-1}$ (■), as a function of the volume fraction

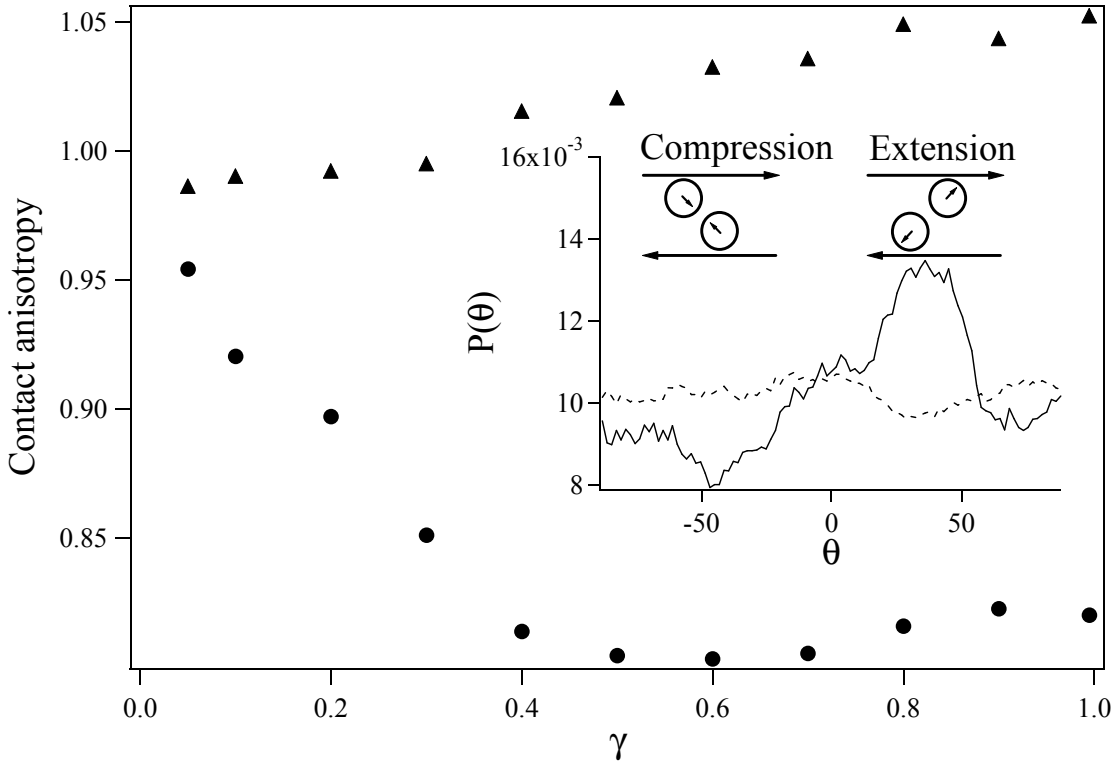

FIG. 3: Ratio of the number contacts in the compression quadrant over the number of contacts in the extension quadrant under shear ($\dot{\gamma} = 3.5.10^{-3}$) as a function of the accumulated deformation. • : $\phi = 20$ % and (▲) : $\phi = 50$ %. *Inset :* angular distribution of the contacts at the highest studied shear amplitude, $\gamma = 0.995$, under shear ($\dot{\gamma} = 3.5.10^{-3}$), and for $\phi = 20$ % (continuous line) and $\phi = 50$ % (dashed line).

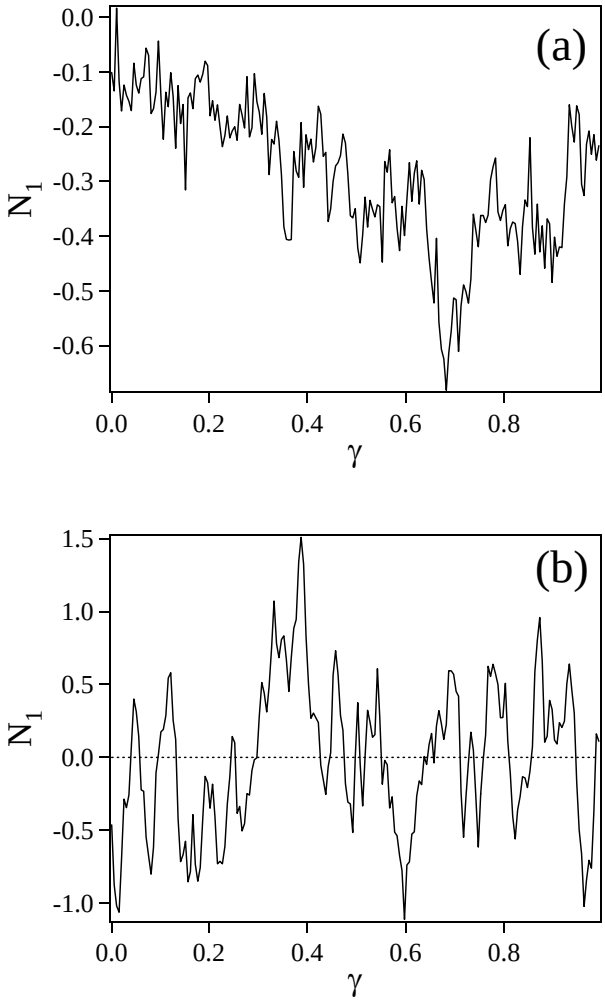

FIG. 4: First normal stress difference as a function of the deformation for suspensions aged $t_w = 1120$. **(a)** : $\phi = 20$ %, **(b)** : $\phi = 50$ %, under the application of shear rate $\dot{\gamma} = 3.5.10^{-3}$.